Leaky wave phenomena of a conductor-back dielectric slab covered with a two-dimensionally electromagnetic band gap superstrate

R. B. Hwang[1]

Received 30 December 2005; revised 23 October 2006; accepted 23 January 2007; published 18 July 2007.

[1] This paper presents the leaky wave phenomena associated with a waveguide structure that consists of a conductor-back dielectric slab covered with a superstrate made up of a two-dimensionally (2-D) electromagnetic band gap (EBG) structure. A guided wave has its energy bounced back and forth between the metallic ground plane and the EBG structure that is taken as a frequency-selective reflection mirror. Because of the finite thickness of the 2-D EBG superstrate, the guided wave will leak or radiate some of its energy into the air region above the waveguide structure to become a leaky wave. By the mode-matching method and the transverse resonance technique, the overall waveguide structure is formulated as a rigorous electromagnetic boundary value problem to yield an exact dispersion relation of the waveguide so that the complex propagation constant of a guided mode can be accurately determined, including the phase and attenuation constants. Additionally, the electric field distribution inside the waveguide and the far-field radiation pattern were also calculated to demonstrate the leaky wave phenomena of this waveguide from a microscopic point of view. On the basis of the excitation of leaky waves, the phenomenology concerning a class of directive antennas with EBG structure as superstrate was clarified in this research.

Citation: Hwang, R. B. (2007), Leaky wave phenomena of a conductor-back dielectric slab covered with a two-dimensionally electromagnetic band gap superstrate, *Radio Sci.*, *42*, RS4010, doi:10.1029/2005RS003445.

1. Introduction

[2] Electromagnetic band gap (EBG) structures were found to have a rich variety of interesting applications in optical and microwave communities in recent years [*Maystre*, 1994; *Nicorovici and McPhedran*, 1994; *Mekis et al.*, 1999; *El-Kady et al.*, 1999]. For instance, the two-dimensionally (2-D) dielectric photonic crystal was employed as a reflection mirror in integrated optics. The metallic periodic structures were utilized in printed circuit board for the suppression of surface wave in order to mitigate the electromagnetic interference problem.

[3] Because of the property of Bragg reflection in a periodic structure, the electromagnetic band gap structure can be employed as a frequency-selective reflection mirror (so-called Bragg mirror). The dielectric parabolic reflector made up of photonic band gap material was employed to reflect and focus the electromagnetic waves [*Thèvenot et al.*, 1999, *Leger et al.*, 2005], such that a high-gain antenna was achieved. An exceptionally directional antenna that was formed by a hybrid combination of a monopole radiation source and a cavity built around a dielectric layer-by-layer three-dimensional photonic crystal was implemented [*Temelkuran et al.*, 2000, *Biswas et al.*, 2001]. Two-dimensionally photonic crystal slabs were employed to design a highly directive light sources [*Fehrembach et al.*, 2001]. A high-gain, low-loss and low-sidelobe antenna made of a woodpile three-dimensional EBG material and a metallic ground plane was developed [*Weily et al.*, 2005]. In addition to the dielectric EBG structure, the metallic EBG structure was also employed to design waveguides or directional antennas [*Poilasne et al.*, 1997, 2000; *Boutayeb et al.*, 2003; *Capolino et al.*, 2005a, 2005b; *Yang and Jackson*, 2000]. With a dipole source placed inside the MPBG (metallic photonic band gap structure) that has some of the metallic wires removed, a directional radiation pattern was obtained [*Poilasne et al.*, 1997, 2000; *Boutayeb et al.*, 2003]. It should be noted that in addition to the

[1]Department of Communication Engineering, National Chiao Tung University, Hsinchu, Taiwan.

0048-6604/07/2005RS003445

antenna applications, the full-wave analysis for the 1-D or 2-D MPBG structure excited by a line source was conducted in general [*Capolino et al.*, 2005b; *Yang and Jackson*, 2000]. An efficient semianalytical algorithm using the array scanning method for the evaluation of the field and mode excitation by a line source embedded in a 2-D metallic EBG waveguide was investigated [*Capolino et al.*, 2005a].

[4] Another application of the electromagnetic band gap superstrates is the design of spatial angular filters for sharpening the radiation pattern of an antenna [*Thèvenot et al.*, 1999; *Zhao et al.*, 2003]. Specifically, the property of localized frequency windows within the stop band, which was due to the irregular components being inserted in the periodic structure, was employed to design an antenna cover for improving the directivity of an antenna [*Lee et al.*, 2005]. The basic concept of this class of applications can be traced back to the work of *Jackson et al.* [1993, 2005] who had used the narrow-beam structure, consisting of dielectric layers of alternating thickness and material constant (1-D periodic layers) stacked over a ground plane, to design a leaky wave antenna. Recently, the radiation characteristics of a 2-D periodic leaky wave antenna made up of a periodic array of metal patches (or slots) on a grounded substrate were investigated [*Zhao et al.*, 2005a, 2005b] with general formulas for the design of 2-D leaky wave antennas [*Zhao et al.*, 2004, 2005c].

[5] In this paper, we replaced the superstrate made up of 1-D periodic layer [*Jackson et al.*, 1993] by a 2-D periodic structure to observe its leaky wave phenomena. Since the two-dimensionally periodic structure has the stop band in two dimensions to reflect the incident wave from an arbitrary incident angle, it should have different leaky wave characteristics compared to those in 1-D periodic case. The structure under consideration can be viewed as a conductor-back dielectric slab with 2-D EBG superstrate made of an array of rectangular dielectric rods immersed in a uniform dielectric medium. Here, the 2-D EBG can be regarded as a finite stack of 1-D periodic layers that are stacked with equal spacing between two neighboring ones. Each periodic layer contains an infinite number of rectangular dielectric rods of infinite length. Alternatively, the structure can be considered as a waveguide with walls made from a 2-D EBG structure and a metal ground plane, respectively. Moreover, because of the frequency-selective reflection characteristic for the 2-D EBG structure, this waveguide shall be a frequency-selective guiding structure accordingly.

[6] Concerning the theoretical analysis, we shall employ the transverse resonance technique to obtain the dispersion relation of the source-free fields supported by the structure; thus the first step is to study the scattering characteristics of the structure under consideration. The scattering characteristics of such a structure can be easily analyzed as a multilayer boundary value problem. Here, we take the building block approach, such that the 2-D EBG structure can be regarded as a stack of unit cells, each consisting of a 1-D periodic layer in junction with a uniform one. By the rigorous mode-matching method, the input-output relation of a unit cell and the field distributions therein can be determined in a straightforward manner. Once cascading the input-output relation of each unit cell and the conductor-back dielectric guiding layer, the reflection characteristic of the overall structure is determined accordingly. Notably, the present method offers a flexible approach to the analysis of 1-D periodic layer with arbitrary profile by utilizing the staircase approximation to model it as a stack of cascaded 1-D periodic layers with different sizes of dielectric rods. In the absence of any incident wave (source-free condition), the existence of a nontrivial solution defines the condition of resonance in the transverse direction of the waveguide; namely, this determines the dispersion characteristics of the waveguide.

[7] On the basis of the exact approach described above, we have developed a computer program and carried out extensive numerical calculations to identify and explain the physical phenomena associated with the type of waveguides with 2-D EBG superstrate (or waveguide wall) of finite thickness. First of all, the band structure of the 2-D EBG was calculated to identify the stop band regions, wherein the 2-D EBG superstrate serves as a reflection mirror to reflect the incident wave. Secondly, the simply parallel-plate waveguide model was employed to enable the approximate dispersion curve to fall into the stop band region. Thus the initial value of the guiding layer thickness was obtained. Finally, by performing the rigorous calculation for the dispersion relation of the waveguide, we can have the exact dispersion curve. If the dispersion curve does not locate in the stop band region, we can fine tune the guiding layer thickness and repeat the above process until the requirement is met.

[8] Because of the finite thickness of the 2-D EBG superstrate, the reflectivity, in fact, is not perfect even it was operated in the stop band region. Accordingly, the power leaks from the waveguide through the 2-D EBG superstrate into free space. The structure therefore becomes a leaky wave antenna. To demonstrate its leaky wave phenomena, the variations on the phase and attenuation constants against frequency were investigated for the conditions with different thicknesses (unit cell numbers) of the 2-D EBG superstrate. In addition, the eigenvectors associated with the dispersion roots, which represent the mode field patterns, were also calculated to demonstrate the far-field radiation (leaky wave) pattern

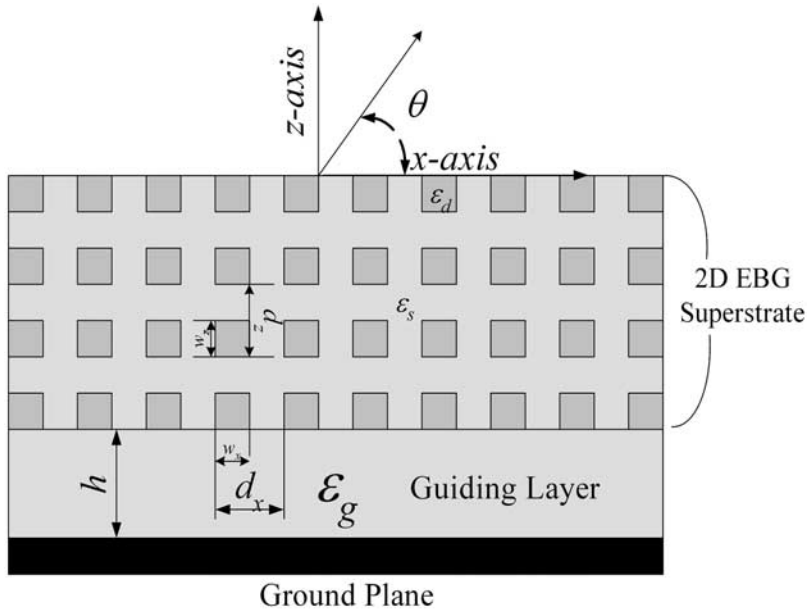

Figure 1. Structure configuration of the leaky wave antenna incorporating a 2-D EBG superstrate. The guiding layer was sandwiched between a metallic ground plane and the 2-D EBG superstrate. The 2-D EBG structure comprises 2-D rectangular dielectric cylinder arrays immersed in a uniform dielectric medium.

and the decaying electric field distribution in the guiding layer, as well. Besides, the characteristics of the radiation main beam angle and bandwidth were examined by the normalized phase and attenuation constants both. These results establish consistently the distinctive characteristics of the waveguide with 2-D EBG superstrate of finite thickness from different viewpoints. In short, the purpose of this research is to systematically and physically explain the phenomenology related to a class of directive antennas, which takes the EBG structure as a superstrate, on the basis of the excitation of leaky waves.

2. Description of the Problem

[9] Figure 1 depicted the structure under consideration, which consists of a conductor-back dielectric slab (or guiding layer) covered with a 2-D EBG superstrate. The 2-D EBG structure has a finite thickness along the z direction, while it extends infinitely along the x and y directions. The 2-D EBG superstrate is made up of rectangular dielectric cylinders array embedded in a uniform host medium. The relative dielectric constants of the cylinder and the host medium are ε_d and ε_s, respectively. The widths of the rectangular dielectric cylinder along the x and z axes are w_x and w_z, respectively. The periods along the x and z direction are respectively designated as d_x and d_z. The guiding layer has the relative dielectric constant ε_g and thickness h.

3. Method of Analysis

[10] As mentioned earlier, the transverse resonance technique was employed in the theoretical analysis to formulate the dispersion relation of the waveguide. The scattering analysis for the overall structure must be formulated first. Since the scattering of plane wave by a stack of 1-D periodic layers has been well developed as a rigorous boundary value problem [*Collin*, 1991; *Peng et al.*, 1975; *Tamir and Zhang*, 1996; *Hwang and Peng*, 2003; *Petersson and Jin*, 2005], the derivation of the input-output relation for a 1-D periodic layer is briefly outlined here while the details could be referred to the literature [*Tamir and Zhang*, 1996; *Hwang and Peng*, 2003]. Specifically, the results in the form of input impedance and transfer matrices will be used as the building block to analyze the plane wave scattering by the stack of periodic layers [*Hall et al.*, 1988; *Peng et al.*, 1975; *Tamir and Zhang*, 1996; *Hwang and Peng*, 2003].

3.1. Input-Output Relation of a 1-D Periodic Layer

[11] The 1-D periodic layer is assumed to be vertically uniform and is characterized by a relative dielectric constant that is periodic along the x direction, given as

$$\varepsilon(x) = \varepsilon(x + d_x), \tag{1}$$

where d_x is the period along the x direction. Because of the spatial periodicity, a set of Fourier components or space harmonics is generated everywhere in the structure; the propagation constant of the nth space harmonic in the x direction is given by

$$k_{xn} = k_x + n\frac{2\pi}{d_x}, \quad \text{for } n = \ldots, -2, -1, 0, 1, 2, \ldots, \tag{2}$$

where k_x is the fundamental wave number along the x direction. On the basis of Floquet's theorem, the general field solutions can be expressed as a superposition of the complete set of space harmonics. With respect to the z direction, the tangential electric and magnetic field solutions in 1-D periodic medium can be written, for the transverse electric (TE) mode, as

$$E_y(x,z) = \sum_{n=-\infty}^{\infty}\sum_{m=-\infty}^{\infty} -Q_{mn}\left[e^{-j\mathbf{k}_{zm}z}c_m + e^{j\mathbf{k}_{zm}z}d_m\right]e^{-jk_{xn}x} \tag{3a}$$

$$H_x(x,z) = \sum_{n=-\infty}^{\infty}\sum_{m=-\infty}^{\infty} P_{mn}\left[e^{-j\mathbf{k}_{zm}z}c_m - e^{j\mathbf{k}_{zm}z}d_m\right]e^{-jk_{xn}x}, \tag{3b}$$

where k_{zm} is the propagation constant along the z direction of the mth mode and is determined [*Peng et al.*, 1975; *Tamir and Zhang*, 1996] from the dispersion relation of the periodic medium for a given k_{xn}, the propagation constant of the nth space harmonic as defined in equation (2). Once k_{zm} is obtained, the Fourier amplitudes, P_{mn} and Q_{mn} can then be determined in a straightforward manner. Parameters c_m and d_m are, respectively, the amplitudes of the forward and backward propagating waves of the mth mode in the 1-D periodic layer.

[12] After collecting the modal amplitude of each space harmonic in (3a) and (3b) and filling in the voltage and current column vectors, we have the two vectors written as follows:

$$\underline{V}(z) = \mathbf{Q}\{\exp(-j\boldsymbol{\kappa}_z z)\underline{c} + \exp(+j\boldsymbol{\kappa}_z z)\underline{d}\} \tag{4a}$$

$$\underline{I}(z) = \mathbf{P}\{\exp(-j\mathbf{k}_z z)\underline{c} - \exp(+j\mathbf{k}_z z)\underline{d}\}, \tag{4b}$$

where $\underline{V}(z)$ and $\underline{I}(z)$ are column vectors, each containing the Fourier components of the electric and magnetic fields in its entry, respectively. The matrix $\mathbf{P}$ and $\mathbf{Q}$ are full matrices with their (m, n)th element defined in equations (3a) and (3b), and $\mathbf{k}_z$ is a diagonal matrix with the propagation constant of the mth space harmonic along the z direction, k_{zm}, as its mth diagonal element. If we denote the output impedance as $\mathbf{Z}_l$, the voltage and current at the output satisfy the condition

$$\underline{V}(z = t) = \mathbf{Z}_l\underline{I}(z = t). \tag{5}$$

Substitution of (5) into (4a) and (4b), we can determine the relation between the amplitude vectors $\underline{c}$ and $\underline{d}$, as

$$\underline{d} = \boldsymbol{\Gamma}\underline{c}\ , \tag{6}$$

where $\boldsymbol{\Gamma}$ is the reflection matrix at the output end, as defined by

$$\boldsymbol{\Gamma} = e^{-j\mathbf{k}_z t}\boldsymbol{\Gamma}_l e^{-j\mathbf{k}_z t} \tag{7}$$

$$\boldsymbol{\Gamma} = (\mathbf{Z}_l\mathbf{P} + \mathbf{Q})^{-1}(\mathbf{Z}_l\mathbf{P} - \mathbf{Q}). \tag{8}$$

Substituting (6), (7) and (8) into (4a) and (4b), we can derive the input impedance matrix, $\mathbf{Z}_{in}$, at the input interface, $z = 0$, which is given below:

$$\underline{V}(z = 0) = \mathbf{Z}_{in}\underline{I}(z = 0) \tag{9a}$$

$$\mathbf{Z}_{in} = \mathbf{Q}(\mathbf{I} + \boldsymbol{\Gamma})(\mathbf{I} - \boldsymbol{\Gamma})^{-1}\mathbf{P}^{-1}. \tag{9b}$$

After some matrix operations, we can determine the relationship of the voltage vector between the input and output interfaces, which is named as the voltage transfer matrix, given as follows:

$$\underline{V}(z = t) = \mathbf{T}\underline{V}(z = 0) \tag{10a}$$

with the shorthand notation

$$\mathbf{T} = \mathbf{Q}[\mathbf{I} + \boldsymbol{\Gamma}_l]\exp(-j\mathbf{k}_z t)(\mathbf{I} + \boldsymbol{\Gamma})^{-1}\mathbf{Q}^{-1}. \tag{10b}$$

Besides, the uniform layer can be regarded as the limiting case of 1-D periodic layer with vanishing periodic variation. The voltage and current vectors of

the waves in a uniform layer are similar to those in (4a) and (4b), while the matrix **P** is simply an identity matrix and **Q** is a diagonal matrix with each element representing the characteristic impedance of each space harmonic in the uniform medium. Parameter $\mathbf{k}_z$ is a diagonal matrix, whose element represents the propagation constant of each space harmonic. The nth element of the matrix $\mathbf{k}_z$ and **Q** are written below:

$$k_{z,n}^{(i)} = \sqrt{k_o^2 \varepsilon_i - (k_x + n2\pi/d_x)^2} \tag{11a}$$

$$Q_n = Z_n^{(a)} = \omega\mu_o / k_{z,n}^{(i)}, \tag{11b}$$

where the index denotes the ith uniform dielectric layer having relative dielectric constant ε_i. Thus the input-output relation of uniform layer will be simply a diagonal matrix and can be derived without difficulty.

3.2. Scattering Characteristics of the Waveguide Structure

[13] With the input-output relation and transfer matrix for a single 1-D periodic layer described above, we may employ successively, from the bottom to the top layer, the input-output relation of a unit cell that consists of a 1-D periodic layer in junction with a uniform one. The termination condition at the bottom surface of the 2-D EBG is a diagonal matrix given below:

$$\mathbf{Z}_l = diag\{z_n\}_{n=-\infty,\ldots,+\infty} \tag{12a}$$

$$\text{with } z_n = j\frac{\omega\mu_o}{\sqrt{k_o^2\varepsilon_g - k_{xn}^2}} \tan\sqrt{k_o^2\varepsilon_g - k_{xn}^2}\,h, \tag{12b}$$

where n is the index of the space harmonic running from negative to positive infinity. Each diagonal element, in (12), represents the input impedance of a uniform transmission line with a shorted circuit at the output end.

[14] With the procedure described above, we can now obtain the input impedance matrix looking downward from the top interface of the structure, $\mathbf{Z}_{dn}$, that is, the relationship between the voltage and current vectors at the reference plane, at $z = 0$ given by

$$\underline{V}(0) = \mathbf{Z}_{dn}\underline{I}(0), \tag{13}$$

where $\underline{V}(0)$ and $\underline{I}(0)$ are infinite column vectors whose entries includes the modal amplitudes of the voltage and current in the incident region, such as air. In terms of the superposition of the incident and reflected waves, these column vectors may be written in the following form:

$$\underline{V}(0) = \mathbf{Z}_a(\underline{a} + \underline{b}) \tag{14a}$$

$$\underline{I}(0) = \underline{a} - \underline{b} \tag{14b}$$

$$\mathbf{Z}_a = diag\left\{Z_n^{(a)}\right\}_{n=-\infty,\ldots,+\infty} \tag{14c}$$

$$Z_n^{(a)} = \omega\mu_o / \sqrt{k_o^2 - (k_x + n2\pi/d_x)^2}, \tag{14d}$$

where the vector $\underline{a}$ and $\underline{b}$ represent the amplitudes of incident and reflected plane waves in air region, respectively. $\mathbf{Z}_a$ is a diagonal matrix with its diagonal element representing the characteristic impedance of each space harmonic along the z direction. Substitution of the boundary condition in (14) into (13), the reflection matrix between the incident and reflected waves, at the input interface of the overall structure, is written as follows.

$$\underline{b} = \mathbf{\Gamma}_a\underline{a} \tag{15a}$$

$$\mathbf{\Gamma}_a = (\mathbf{Z}_{dn} + \mathbf{Z}_a)^{-1}(\mathbf{Z}_{dn} - \mathbf{Z}_a), \tag{15b}$$

where $\mathbf{\Gamma}_a$ is the reflection matrix of the overall structure. Thus the reflected amplitudes of all the space harmonics are now completely determined. We then obtain the voltage and current waves over the input surface by (14a) and (14b). Furthermore, we can successively employ the transfer matrix of a unit cell, 10(b), from the top to bottom layer to obtain the electric and magnetic fields everywhere within the structure under consideration.

3.3. Guiding Characteristics of the Waveguide: Source-Free Solutions

[15] In the absence of any incident wave, $\underline{a} = 0$, and the existence of nontrivial solutions requires the condition:

$$\det[\mathbf{Z}_{dn}(k_x, k_o) + \mathbf{Z}_a(k_x, k_o)] = 0, \tag{16}$$

which is known as the transverse resonance condition, and defines the dispersion relation of the waveguide. Notably, (16) depends on the structure parameters, propagation constant along the x direction, k_x, and the free-space wave number (or frequency). For a fixed

frequency, we can obtain k_x, which is generally a complex number with the real and imaginary parts representing the phase and attenuation constants along the waveguide axis (x axis). Such a determinantal equation of infinite order must be truncated to a finite one for numerical analysis. We have implemented a computer code on the basis of the exact formulation described above to determine the dispersion root of the waveguide. Extensive results have systematically obtained for various structural parameters, in order to identify the wave propagation phenomena and their physical implications.

3.4. Band Structure of a Two-Dimensionally Periodic Medium

[16] Although the 2-D EBG superstrate is finite in its thickness, the stop band behavior can be understood by the band structure of the corresponding infinite 2-D EBG. This can be achieved by imposing the periodic boundary (or Bloch) condition along the z axis; that is, a wave traveling through a period d_z along the z direction experiences a phase delay, $\exp(-jk_z d_z)$, satisfies the equation

$$\underline{V}(z + d_z) = e^{-jk_z d_z}\underline{V}(z). \tag{17a}$$

Equation (17a) can be further converted into an eigenvalue problem with the eigenvalues representing the z direction propagation constants in an infinitely 2-D periodic medium, as given in (17b).

$$\mathbf{T}_{EBG}(w_z) \cdot \mathbf{T}_u(d_z - w_z)\underline{V}(z) = e^{-jk_z d_z}\underline{V}(z), \tag{17b}$$

where the matrices $\mathbf{T}_{EBG}$ and $\mathbf{T}_u$ respectively denote the transfer matrix through 1-D periodic layer and uniform layer. Therefore we could determine the relationship among the three parameters: k_x, k_z and k_o, of which any desired parameter may be determined for a given set of the two parameters. For example, if the incident condition is specified for the component of k_x under a certain frequency of operation, we can determine the value of k_z by solving the eigenvalue in (17b). With k_o fixed, the relationship between k_x and k_z is referred to as the phase relation; on the other hand, with k_x fixed, relationship between k_o and k_z defines as the dispersion relation. In general, k_z is a complex number; its real and imaginary parts represent the phase and attenuation constants of the wave propagating along the z direction. On the other hand, we can also have the value of k_x for a given incident condition k_z, by exchanging the variable x with z. Through the rigorous analysis presented so far, we have derived the phase relation of the waves propagating in such a class of 2-D periodic medium.

4. Design Criterion for Choosing the Structure Parameters: Band Structure Calculation for the 2-D EBG Superstrate in Infinite Extent

[17] Before embarking on an elaborate numerical analysis; in particular for the dispersion relation of the waveguide, it is necessary to understand the reflection characteristics in conjunction with the 2-D EBG superstrate since it acts as a reflection mirror. We first assumed that the 2-D EBG structure extends infinitely along the z direction. By solving the eigenvalue problem in (17b), we could determine the phase relation of the waves propagating in the 2-D EBG medium. This phase relation defines the relation among k_o, k_x and k_z (here we assumed $k_y = 0$). For example, when the parameters k_o and k_x are given, the propagation constant along the z direction, k_z could be determined. If the k_z is a real number, the wave is propagating along the z direction. On the contrary, it experiences reflection along the z direction if the parameter k_z is a complex number. Consequently, the band structure (or phase relation) for the 2-D EBG medium was established to allocate the frequency range of the stop bands.

[18] The structure parameters employed in the following numerical calculations were given below. The relative dielectric constants of the dielectric rod and the surrounding medium are $\varepsilon_d = 10.2$ and $\varepsilon_s = 1.03$. The guiding layer and uniform surrounding medium shares the same relative dielectric constant $\varepsilon_s = \varepsilon_g = 1.03$. The square dielectric rod has the width $w_x = w_z = 0.5d_x$. The period along the x direction was designated as d_x. The period along the z axis is set to $d_z = d_x$.

[19] Figure 2 shows the band structure for the 2-D EBG of infinite extent. The normalized propagation constant (k_z/k_o) is plotted against the normalized phase constant (k_x/k_o) under the condition of $k_y = 0$. Those curves with real k_z/k_o are marked with black dots; therefore the apparently black regions represent the passbands, wherein the wave is propagating along the z direction. Consequently, the remaining regions in white color represent the stop bands, wherein the wave experience reflection. Notably, in the first white zone between two dash lines, the 2-D EBG medium has a *complete* stop band for the normalized phase constant, k_x/k_o, ranging from zero to unity. Within this complete stop band, the 2-D EBG structure is able to reflect the incident waves with arbitrary incident angles. Such a 2-D EBG medium, along with the metallic ground plane, allows the wave to bounce back and forth and propagate along the x direction in the guiding layer. Therefore the

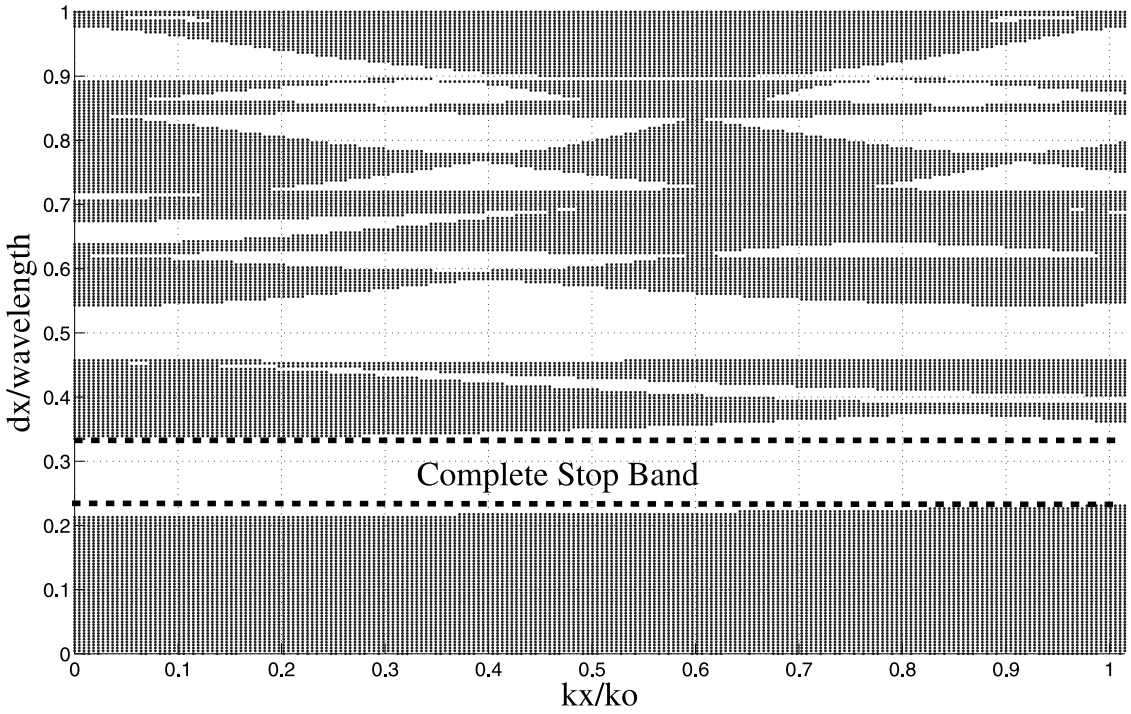

Figure 2. Band structure (phase relation) for a 2-D EBG structure of infinite extent with TE polarization.

waveguide is extremely similar to a parallel-plate waveguide. It is instructive to consider first the approximation of the dispersion relation by that of a ''reference'' parallel-plate waveguide. The dispersion relation of the nth parallel-plate waveguide mode is given as

$$k_x/k_o = \sqrt{\varepsilon_g - \left(\frac{n\lambda}{2h_{eff}}\right)^2}. \tag{18a}$$

For example, the cutoff wavelength for the parallel-plate waveguide mode with $n = 1$ is given below:

$$\lambda_c^{(n=1)} = 2h_{eff}\sqrt{\varepsilon_g}\ , \tag{18b}$$

where the parameter h_{eff} is the effective width of the parallel-plate waveguide. Conceivably, the effective width, h_{eff}, should be greater than that of the guiding layer thickness h, because the incident wave, in fact, penetrates into the 2-D EBG superstrate, resulting in the so-called Goos-Hanchen shift. Although the actual width of the waveguide may differ from h, we could use it as an initial value to approximately figure out the cutoff frequency. Since the waveguide must be operated in the frequency range where the 2-D EBG wall is working in the stop band, we chose $d_x/\lambda_c^{(n=1)} = 0.25$ to allow the cutoff frequency to fall within the complete stop band, as indicated in Figure 2. Therefore the initial design parameter for the guiding layer thickness was designated

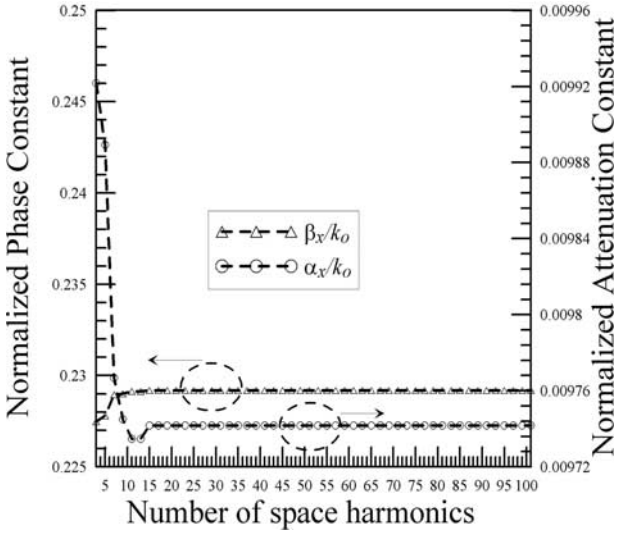

Figure 3. Convergence test for the number of space harmonics employed in calculating the dispersion roots.

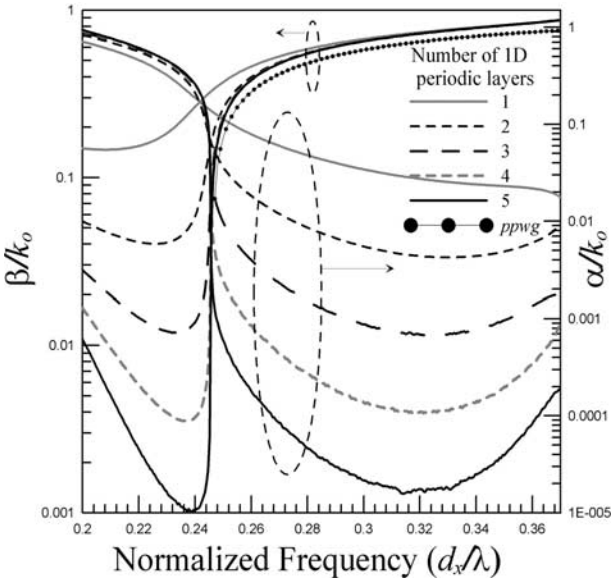

Figure 4. Variation of the dispersion roots, including the normalized phase and attenuation constants, of the waveguide against normalized frequency with the width of guiding layer $h = 2d_x$; the number of 1-D periodic structure (2-D EBG waveguide wall) was changed from one to five.

as $h = 2d_x/\sqrt{\varepsilon_g}$. The h approaches $2d_x$ because ε_g is near unity.

5. Numerical Results and Discussion

5.1. Convergence Test for the Number of Space Harmonics Employed

[20] Before carrying out extensive numerical calculations, we had performed the convergence test for the dispersion root against the number of space harmonics employed to ensure the accuracy of our computer simulations. Figure 3 depicts the variation of dispersion roots, including the normalized phase (β_x/k_o) and attenuation (α_x/k_o) constants, against the number of space harmonics employed, ranging from 3 to 101 with the normalized frequency $d_x/\lambda = 0.25$. The space harmonics includes vertically evanescent modes and the criterion for choosing the number of space harmonics follows the rule given by *Tamir and Zhang* [1996]. It is evident that the normalized phase and attenuation constants rapidly converge to certain values as the number of space harmonics exceeds 19. Throughout this paper, the remaining numerical simulation examples were carried out using 19 space harmonics.

5.2. Dispersion Relation of the Waveguide

[21] Figure 4 illustrates the variation on the dispersion characteristics, including the normalized phase and attenuation constants, against the normalized frequency for various thicknesses of the 2-D EBG superstrate (or numbers of 1-D periodic layers). The curves corresponding to the axis on the left represent the normalized phase constant (β_x/k_o), while those corresponding to axis on the right are the normalized attenuation constant (α_x/k_o). From Figure 4, we can observe that the normalized phase and attenuation constants have drastic changes as the normalized frequency is near $d_x/\lambda = 0.245$. Below this frequency, the normalized attenuation increases rapidly, while the phase constant decreases to a small value. For easy comparison, we plotted the phase constant distribution for a "reference" metallic parallel-plate waveguide with width h. The phase constant distribution is plotted in Figure 4 by a solid line marked with circles. The normalized cutoff frequency of this reference waveguide is $d_x/\lambda_c = 0.2463$. It is noted that the dispersion curves of the 2-D EBG waveguide follow closely that of the "reference" parallel-plate waveguide, except for a slight shift in its position. We may infer that it is due to the Goos-Hanchen shift as described previously.

[22] Moreover, above the normalized frequency $d_x/\lambda = 0.245$, the attenuation constant started to decrease until $d_x/\lambda \cong 0.32$. Recalling the band structure in Figure 2, the 2-D EBG structure was operated in the complete stop band as the normalized frequency falls into the region in the vicinity of $d_x/\lambda \cong 0.3$. This consistently confirms the calculation for the band structure and the dispersion relation of the waveguide. Besides, the increase in the

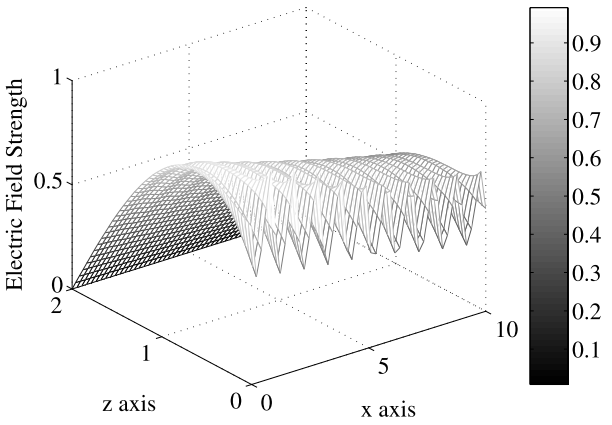

Figure 5. Contour plot of the tangential electric field strength (E_y) within the guiding layer ($0 \le z \le h$). The number of the 1-D periodic structure is three, and the structure parameters are the same as the previous case. The normalized frequency is $d_x/\lambda = 0.38$.

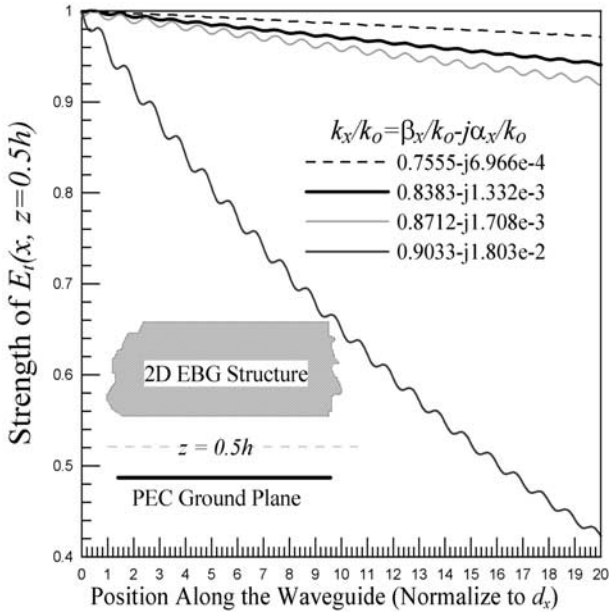

Figure 6. Distribution of the tangential electric field strength against the position along the x direction for various operation conditions.

number of 1-D periodic layers definitely enhance the reflectivity of 2-D EBG wall, leading to the decrease in the attenuation constant, as indicated in Figure 4.

5.3. Tangential Electric Field Distribution Along the Waveguide

[23] From the previous example, we know that the dispersion curve of the leaky waveguide is extremely similar to that of a metallic parallel-plate waveguide. In this example, we plotted the contour map for the strength of the tangential electric field component $E_y(x, z)$, with the maximum field strength normalized to unity, within the guiding layer for further inspection of the physical consequences. As shown in Figure 5, we observe that the maximum field strength occurs around the center of the guiding layer, while it is zero at $z = h$, the plane on the metal ground plane, owing to the vanishing of tangential electric field on the metal ground plane (a perfect electric conductor). The electric field distribution is similar to the first-order parallel-plate waveguide mode with the field pattern, such as, $E_o\sin(\pi x/h_{eff})$. However, the electric field does not vanish at the boundary between guiding layer and 2-D EBG superstrate, and this will allow the waveguide to leaks its energy from the guiding layer through the finite 2-D EBG superstrate into air region above structure. It is interesting to note that the field pattern in the EBG region varies periodically in accordance to the periodic variation of structure, as expected.

[24] Moreover, we plotted the strength of the electric field component $E_y(x, z = 0.5h)$ along the center of the waveguide, shown in Figure 6. The vertical axis represents the strength of the electric field, while the horizontal one is the position along the guide axis, running from zero to $20d_x$. The electric field distributions were calculated on the basis of the eigenvectors corresponding to the dispersion roots (eigenvalues) shown in Figure 4. The normalized phase and attenuation constants of the four dispersion roots are attached in Figure 6, with the respective normalized frequencies, $d_x/\lambda = 0.35$, 0.36, 0.37 and 0.38. The filed distributions interestingly exhibited a decaying standing wave along guide axis. The first case exhibited the slowest decay among the four cases because of its smallest attenuation constant. Conversely, the fourth case had the strongest attenuation since its attenuation constant is the largest one among the four cases.

5.4. Leaky Wave Radiation Pattern

[25] From the previous example, we know that the normalized phase constants along the longitudinal x direction is less than unity ($\beta_x/k_o < 1$), so that a wave in the air region may propagate in the transverse direction. Therefore the waveguide with the EBG superstrate can leak (or radiate) its energy into the air

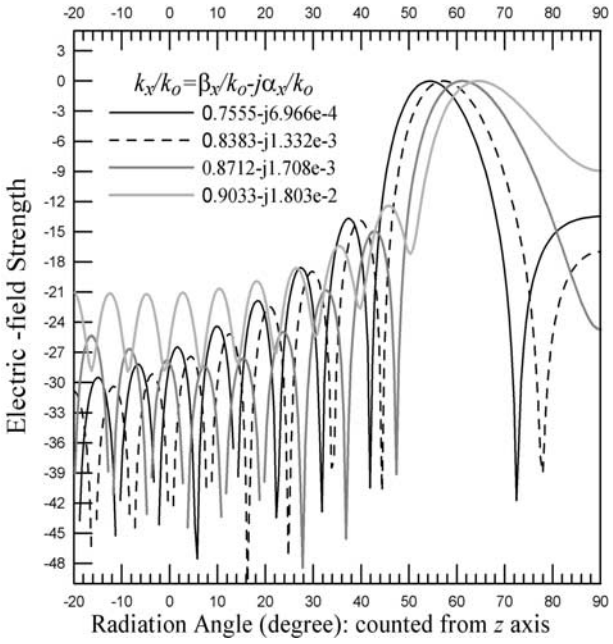

Figure 7. Radiation pattern for the leaky wave antenna, with the normalized propagation constants given in the legend.

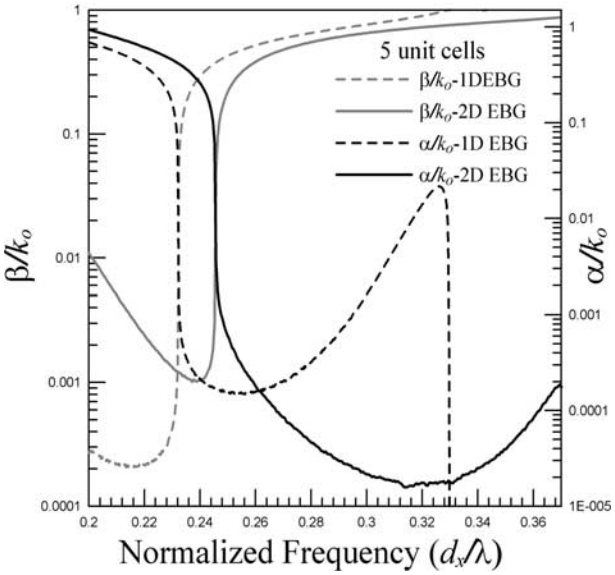

Figure 8. Dispersion relations of the waveguide with 1-D EBG and 2-D EBG walls. The waveguide with 2-D EBG wall has five 1-D periodic layers, and the structure configuration is the same as described in Figure 3. While the waveguide with 1-D EBG also contains five unit cells, the 1-D periodic layer was replaced with a uniform dielectric layer with relative dielectric constant 10.2.

region and becomes a leaky wave structure. To demonstrate the leaky wave phenomena of the waveguide structure under consideration, we calculated the radiation far-field patterns and plotted them in Figure 7. The four dispersion roots were again employed to calculate the electric and magnetic fields (eigenvectors) on the output surface of the 2-D EBG superstrate. Here, the antenna length was assumed to be $20d_x$. On the basis of the equivalent principle, we could calculate the far-field radiation pattern by the equivalent electric and magnetic currents on the outer surface of the 2-D EBG superstrate. It is noted that in the far-field calculations, we have neglected the edge condition associated with the structure of finite length.

[26] As is well known for a leaky wave, its radiation angle can be predicted by using the formula: $\theta \cong \sin^{-1}(\beta_x/k_o)$, where β_x is the phase constant along the guide axis. Figure 7 shows that the radiation angles of the main beam for the four cases of propagation constants are at around 54.21°, 56.96°, 60.60°, and 64.59°, respectively,. These radiation angles agree with the estimated values from the phase constants, and they swings as the frequency changes. The beam width increased in accordance with the increase in the normalized attenuation constant, which confirms the property of conventional leaky wave antennas. For practical design, the sidelobe level in the radiation pattern can be reduced by tapering the 2-D EBG wall at its input and output ends to reduce the reflection of incident waves at the two ends. It can be implemented by tapering the aspect ratio (w_x/d_x) of the 1-D periodic layers.

[27] The field distribution plotted in Figure 7 is based on the source-free fields supported by the structure under consideration, such that the radiation far-field contributed by the space wave was neglected in our research. It is noted that other authors [*Capolino et al.*, 2005a] compared the total field (including space contributions as well as modal (leaky wave) contributions) with the modal contribution; they show that the space wave contribution is negligible. Besides, another theory [*Capolino et al.*, 2005b] presented can also be applied to this waveguide case with the same conclusion.

5.5. Dispersion Relations of the Waveguide With 1-D EBG and 2-D EBG Wall

[28] As we have described in the introduction, the class of 2-D EBG antennas was evolved from the structure proposed in the literature [*Jackson et al.*, 1993; *Thèvenot et al.*, 1999], the conductor-back dielectric slab waveguide with alternating homogeneous dielectric layers (or 1-D EBG superstrate) is taken as the top cover of the dielectric waveguide. The 1-D or 2-D EBG superstrate utilized here both, in fact, are acted as a reflection mirror to sustain a parallel-plate-like waveguide. However, the following example, which deals with the dispersion relation of the waveguide with 1-D and 2-D EBG superstrate, to be demonstrated is for understanding the difference in leaky wave characteristics between the 1-D and 2-D EBG superstrate.

[29] In Figure 8, the vertical axis on the left corresponds to the normalized phase constant, while that on the right is for the normalized attenuation constant. The variations on the phase (and attenuation) constants for the two cases are similar to each other. For the waveguide with 1-D EBG superstrate, when the normalized frequency is above 0.328, the phase constant enters into the bound-wave region with the normalized phase constant greater than unity; wherein the field is bound to the structure and becomes a surface wave with zero attenuation constant (the dielectric media are assumed to be lossless). Besides, as shown in Figure 8, these two dispersion curves exhibit cutoff phenomenon. However, the normalized cutoff frequency for 1-D EBG case is lower than that of the 2-D EBG case. From the physical picture of wave phenomenon, it is instructive to know that the wave is bouncing vertically as the operation frequency is near the cutoff frequency. Under this situation, the wave is normally incident into the superstrate. Since the 1-D EBG superstrate has the higher average dielectric constant compared with that of the 2-D EBG

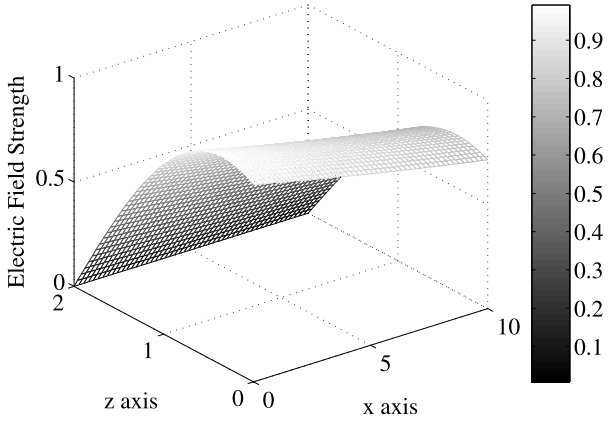

Figure 9. Tangential electric field pattern within the guiding layer. The waveguide wall is made up of 1-D EBG; its structure parameters are the same as the previous case. The operation normalized frequency is equal to 0.32. The normalized propagation constant along the x direction is $0.898 - j0.01401$.

superstrate, the 1-D EBG case certainly have stronger reflection than that of the 2-D EBG case. On the other hand, as the normalized frequency is increasing, the incident angle will change gradually from vertical to horizontal direction. In this case, it may be viewed as oblique incident into the superstrate. We know that the reflection coefficient for a wave incident into a 1-D periodic layer is decreasing as the incident angle is increasing. Conversely, from the band structure depicted in Figure 2, the 2-D EBG has a wide stop band for the incident wave even with large incident angle (or the value of $k_x/k_o = \sin\theta_{inc}$ is considerably large). Such that in Figure 8, it is apparently to see the leaky wave region ($\beta < k_o$ and $\alpha > 0$ excluding the below cutoff condition) for the 2-D EBG superstrate is wider than that of the 1-D EBG superstrate.

5.6. Tangential Electric Field Pattern Within the Guiding Layer: 1-D EBG Case

[30] In addition to the calculation of dispersion relation shown in the previous example, we also compute the tangential electrical field distribution within the guiding layer for the leaky wave structure with 1-D EBG superstrate. The structure parameters are the same as those of the last example. The normalized frequency and the propagation constant along the wave-guiding direction are 0.32 and $0.898 - j0.01401$, respectively. From Figure 8, we observe that the electric field strength is decaying along the wave-guiding direction owing to the attenuation constant. Comparing Figure 8 with Figure 5, it is interesting to see that the periodic variation in the electric field distribution along the guide axis disappears, as shown in Figure 9, because of no periodicity in the x direction.

6. Conclusion

[31] This paper dealt with the guiding characteristics of a conductor-back dielectric layer covered with a superstrate made up of 2-D EBG structure. Such a class of structures has also been widely studied experimentally and numerically, and employed as a directive antenna with narrow beam width, known as the Fabry-Perot cavity (or resonant) antenna. We systematically analyze this structure by using the rigorous mode-matching method incorporating the transverse resonance technique to determine the dispersion relation of the source-free fields supported by the structure. From the dispersion characteristics, we know that the guiding characteristic of this waveguide is extremely similar to that of a parallel-plate waveguide, when the 2-D EBG structure was operated in stop band. However, because of the finite thickness of the 2-D EBG structure, it leaks energy from the guiding layer through the 2-D EBG structure into the surrounding medium (air), resulting a high-directivity radiation pattern (leaky wave). The main contribution of this research is to clarify the physical insight with respect to the class of directive antennas based on the excitation of leaky waves.

[32] **Acknowledgments.** The author acknowledges Song-Tsuen Peng, National Chiao Tung University, Hsinchu, Taiwan, and T. Tamir and Ming Leung, Polytechnic University, New York, United States, for mentoring in the area of periodic waveguide, consistent encouragement,and valuable comments in revising this manuscript. This research was sponsored in part by MOE ATU Program, Taiwan, and National Science Council under contract NSC 95-2221-E-009-045-MY3.

References

Biswas, R., E. Ozbay, B. Temelkuran, M. Bayindir, M. M. Sigalas, and K.-M. Ho (2001), Exceptionally directional sources with photonic-bandgap crystals, *J. Opt. Soc. Am. B Opt. Phys.*, *18*(11), 1684–1689.

Boutayeb, H., K. Mahdjoubi, and A. C. Tarot (2003), Analysis of radius-periodic cylindrical structures, *Proc. IEEE Antennas Propag. Soc. Int. Symp. Dig.*, *2*, 813–816.

Capolino, F., D. R. Jackson, and D. R. Wilton (2005a), Mode excitation from sources in two-dimensional EBG waveguides using the array scanning method, *IEEE Microwave Wireless Components Lett.*, *15*(2), 49–51.

Capolino, F., D. R. Jackson, and D. R. Wilton (2005b), Fundamental properties of the field at the interface between air and a periodic artificial material excited by a line source, *IEEE Trans. Antennas Propag.*, *53*(1), 91–99.

Collin, R. E. (1991), Periodic structures, in *Field Theory of Guided Waves*, 2nd ed., chap. 9, pp. 605–641, IEEE Press, Piscataway, N. J.

El-Kady, I., M. Sigalas, R. Biswas, and K. Ho (1999), Dielectric waveguides in two dimensional photonic band-gap materials, *J. Lightwave Technol.*, *17*, 2042–2049.

Fehrembach, A., S. Enoch, and A. Sentenac (2001), Highly directive light sources using two-dimensional photonic crystal slabs, *Appl. Phys. Lett.*, *79*, 4280–4282.

Hall, R. C., R. Mittra, and K. M. Mitzner (1988), Analysis of multilayered periodic structures using generalized scattering matrix theory, *IEEE Trans. Antennas Propag.*, *36*(4), 511–517.

Hwang, R. B., and S. T. Peng (2003), Scattering and guiding characteristics of waveguides with two-dimensionally periodic walls of finite thickness, *Radio Sci.*, *38*(5), 1091, doi:10.1029/2002RS002847.

Jackson, D. R., A. A. Oliner, and A. Ip (1993), Leaky-wave propagation and radiation for a narrow-beam multiple-layer dielectric structure, *IEEE Trans. Antennas Propag.*, *41*(3), 344–348.

Jackson, D. R., A. A. Oliner, T. Zhao, and J. T. Williams (2005), Beaming of light at broadside through a subwavelength hole: Leaky wave model and open stopband effect, *Radio Sci.*, *40*, RS6S10, doi:10.1029/2004RS003226.

Lee, Y., J. Yeo, R. Mittra, and W. Park (2005), Application of electromagnetic bandgap (EBG) superstrates with controllable defects for a class of patch antennas as spatial angular filters, *IEEE Trans. Antennas Propag.*, *53*(1), 224–235.

Leger, L., T. Monediere, and B. Jecko (2005), Enhancement of gain and radiation bandwidth for a planar 1-D EBG antenna, *IEEE Microwave Wireless Components Lett.*, *15*(9), 573–575.

Maystre, D. (1994), Electromagnetic study of photonic band gaps, *Pure Appl. Opt.*, *3*, 975–993.

Mekis, A., S. Fan, and J. D. Joannopoulos (1999), Absorbing boundary conditions for FDTD simulations of photonic crystal waveguides, *IEEE Microwave Guided Wave Lett.*, *9*, 502–504.

Nicorovici, N. A., and R. C. McPhedran (1994), Lattice sums of off-axis electromagnetic scattering by gratings, *Phys. Rev. E*, *50*, 3143–3160.

Peng, S. T., T. Tamir, and H. L. Bertoni (1975), Theory of dielectric grating waveguides, *IEEE Trans. Microwave Theory Tech.*, *23*, 123–133.

Petersson, L. E. R., and J.-M. Jin (2005), A two-dimensional time-domain finite element formulation for periodic structure, *IEEE Trans. Antennas Propag.*, *53*(4), 1480–1488.

Poilasne, G., J. Lenormand, P. Pouliquen, K. Mahdjoubi, C. Terret, and P. Gelin (1997), Theoretical study of interactions between antennas and metallic photonic band-gap materials, *Microwave Opt. Technol. Lett.*, *15*, 384–389.

Poilasne, G., P. Pouliquen, K. Mahdjoubi, L. Desclos, and C. Terret (2000), Active metallicphotonic bandgap material MPBG: Experimental results on beam shaper, *IEEE Trans. Antennas Propag.*, *48*(1), 117–119.

Tamir, T., and S. Zhang (1996), Modal transmission-line theory of multilayered grating structures, *J. Lightwave Technol.*, *14*, 94–927.

Temelkuran, B., M. Bayindir, E. Ozbay, R. Biswas, M. M. Sigalas, G. Tuttle, and K. M. Ho (2000), Photonic crystal-based resonant antenna with a very high directivity, *J. Appl. Phys.*, *87*, 603–605.

Thèvenot, M., C. Cheype, A. Reineix, and B. Jecko (1999), Directive photonic-bandgap antennas, *IEEE Trans. Microwave Theory Tech.*, *47*, 2115–2122.

Weily, A. R., L. Horvath, K. P. Esselle, B. C. Sanders, and T. S. Bird (2005), A planar resonator antenna based on a woodpile EBG material, *IEEE Trans. Antennas Propag.*, *53*(1), 216–223.

Yang, H.-Y. D., and D. R. Jackson (2000), Theory of line-source radiation from a metal-strip grating dielectric-slab structure, *IEEE Trans. Antennas Propag.*, *48*(4), 556–564.

Zhao, T., D. R. Jackson, J. T. Williams, and A. A. Oliner (2003), General formulas for a 2D leaky-wave antenna, *IEEE Antennas Propag. Soc. Int. Symp.*, *2*, 1134–1137.

Zhao, T., D. R. Jackson, J. T. Williams, and A. A. Oliner (2004), Simple CAD model for a dielectric leaky-wave antenna, *IEEE Antennas Wireless Propag. Lett.*, *3*, 243–245.

Zhao, T., D. R. Jackson, J. T. Williams, H.-Y. D. Yang, and A. A. Oliner (2005a), 2-D periodic leaky–wave antennas—Part I: Metal patch design, *IEEE Trans. Antennas Propag.*, *53*(11), 3505–3514.

Zhao, T., D. R. Jackson, and J. T. Williams (2005b), 2–D periodic leaky–wave antennas—Part II: Slot design, *IEEE Trans. Antennas Propag.*, *53*(11), 3515–3524.

Zhao, T., D. R. Jackson, J. T. Williams, and A. A. Oliner (2005c), General formulas for 2-D leaky-wave antennas, *IEEE Trans. Antennas Propag.*, *53*(11), 3525–3533.

R. B. Hwang, Department of Communication Engineering, National Chiao Tung University, 1001 Ta-Hsueh Road, Hsinchu, Taiwan. (raybeam@mail.nctu.edu.tw)